Chin.J.Geochem.(2012)31:120–127
DOI: 10.1007/s11631-012-0558-2

Geochemical and stable isotopic studies of Gulf of Suez's hot springs, Egypt

Mohamed Abdel Zaher[1, 2*], Hakim Saibi[3], and Sachio Ehara[1]

[1] *Laboratory of Geothermics, Department of Earth Resources Engineering, Faculty of Engineering, Kyushu University, 744 Motooka, Nishi-ku, Fukuoka 819-0395, Japan*

[2] *Nathional Research Institute of Astronomy and Geophysics, Egypt*

[3] *Laboratory of Exploration Geophysics, Department of Earth Resources Engineering, Faculty of Engineering, Kyushu University, 744 Motooka, Nishi-ku, Fukuoka 819-0395, Japan*

** Corresponding author, E-mail: moh_zaher@yahoo.com*

Received November 23, 2010; accepted December 25, 2010

Abstract The Gulf of Suez region is one of the most interesting geothermal areas in Egypt because of the high temperatures of its springs. The eastern and western shores of the Gulf of Suez are characterized by superficial thermal manifestations including a cluster of hot springs with varied temperatures. Variations of deuterium and oxygen-18 concentrations in thermal waters have been used to aid in describing the source of recharge in the Gulf of Suez hot springs. Isotope and geochemical data for the Gulf of Suez thermal waters suggest that recharge to the hot springs may not be entirely from the Gulf of Suez water, but possibly from the meteoric water that comes from areas of higher altitude surrounding the hot springs.

Key words Gulf of Suez; hot spring; isotope; deuterium; oxygen-18

1 Introduction

Egypt is bounded to the east by what has been interpreted as a median spreading center in the Red Sea and Gulf of Suez (McKenzie et al., 1970) and may reflect the importance of these areas for geothermal development. The most promising areas for geothermal development in the NW Red Sea-Gulf of Suez rift system are locations along the eastern shore of the Gulf of Suez that are characterized by surface thermal manifestations, including a cluster of hot springs with varied temperatures (Fig. 1).

The studied areas including Ain Sokhna (western coast of the gulf), Ayun Musa, Hammam Faraun, and Hammam Musa (eastern coast of the gulf) are considered as the main hot springs in Egypt. The heat for these springs is probably derived from high heat flow and deep circulation controlled by faults associated with the opening of the Red Sea and the Gulf of Suez rifts (Morgan et al., 1983). The isotope and chemical compositions of the thermal waters were used to determine the origin of geothermal waters, in particular to distinguish between meteoric and sea water (Davisson et al., 1994). Previous studies have been conducted on the chemical and isotopic composition of geothermal waters of the Gulf of Suez region (Issar et al., 1971; Himida et al., 1972; El Kiki et al., 1978; Morgan et al., 1983; Shata, 1990; Sturchio and Arehart, 1996).

This study presents the reanalyzes of the chemical compositions of thermal waters that made by (Sturchio and Arehart, 1996). Also, stable isotopic compositions (^{18}O and ^{2}H) of major geothermal water where thermal waters were collected from both sides of the Gulf of Suez.

2 Geological and structure setting

The Red Sea occupies part of a large rift valley in the continental crust of Africa and Arabia. This break in the crust is part of a complex rift system that includes the East African Rift System (Said, 1962). To the north, the Red Sea bifurcates into the Gulfs of Suez and Aquaba, with the Sinai Peninsula in between. The Gulf of Suez is a failed intercontinental rift that forms the NW-SE trending continuation of the Red Sea rift system and was initiated during the late Oligocene to Early Miocene by the NE-SW separation of the African and Arabian plates (Colletta et al., 1988; Patton et al., 1994). It extends more than 300 km in length and can be divided into three parts: the northern portion of the Gulf dips to the SW; the central part dips to the NE; and the southern part dips to the SW. The structure of the Gulf of Suez region is

governed by normal faults and tilted blocks, of which the crests represent a major hydrocarbon exploration target. The faults can be divided into two major sets based on trend. The first set is longitudinally parallel to the axis of the rift being created in an extensional regime during the Neogene. The second consists of transverse faults with dominant N-S to NE-SW trends that inherited passive discontinuities in the Precambrian basement rock (Colletta et al., 1988). Fig. 2 shows a stratigraphic and structural cross section of the central Gulf of Suez. The stratigraphic record of the Gulf of Suez shows that the Gulf existed as a shallow embayment of Tethys as early as the Carboniferous and that a landmass lay at its southern end until the late Cretaceous. The predominantly clastic sediments that characterize its early history transitioned to calcareous marine sediments in the Cenomanian. Igneous rocks younger than Precambrian in the Sinai and neighboring areas are predominantly basaltic dikes and flows of Mesozoic (Meneisy and Kreuzer, 1974) and Oligocene to Lower Miocene age (Siedner, 1973). Their main direction is parallel to the Suez and Red Sea rifts. The rift stratigraphy and related tectonics are well documented (e.g. Garfunkel and Bartov, 1977; Sellwood and Netherwood, 1984; Evans, 1988; Patton et al., 1994; Schütz, 1994).

3 Hot water chemistry

Details of chemical and isotopic studies in the areas around the Gulf of Suez were made by Sturchio et al. (1996). The studied areas, including Ain Sokhna, Ayun Musa, Hammam Faraun, and Hammam Musa, are considered as the main hot springs in Egypt. Results of chemical analyses of thermal waters (Table 1) indicate derivation of solutes mainly from regional marine sedimentary rocks and windblown deposits (marine aerosol and evaporate dust). We find that the most abundant solutes in all thermal waters are Na and Cl, while Mg, Ca, and SO_4 are also prominent. The pH values are near neutral. The total dissolved solids range from 2600 to 14000 mg/L.

Chloride variation diagrams for Gulf of Suez thermal waters (Hammam Faraun, Hammam Musa, Ayoun Musa and Ain Sokhna) were made and compared with the sea water dilution line. The comparison helped us in discussing the origin of these thermal waters. Fig. 3(A) shows the relation between Na concentration and Cl concentration in mg/L based on the chemical analysis in Table 1. The solute concentration being below the seawater dilution line in the plot reflects that some Na may have been lost owing to water-rock interaction within the reservoir. The thermal waters are also enriched in SO_4 relative to the water dilution line except Hammam Faraun hot water (Fig. 3B). This may be due to the derivation of Ca from the dissolution of gypsum in these areas. Fig. 3(C) shows the enrichment of all thermal waters and the maximum percentage of Ca is recorded in the Hammam Faraun hot spring. This implies dissolution of Ca

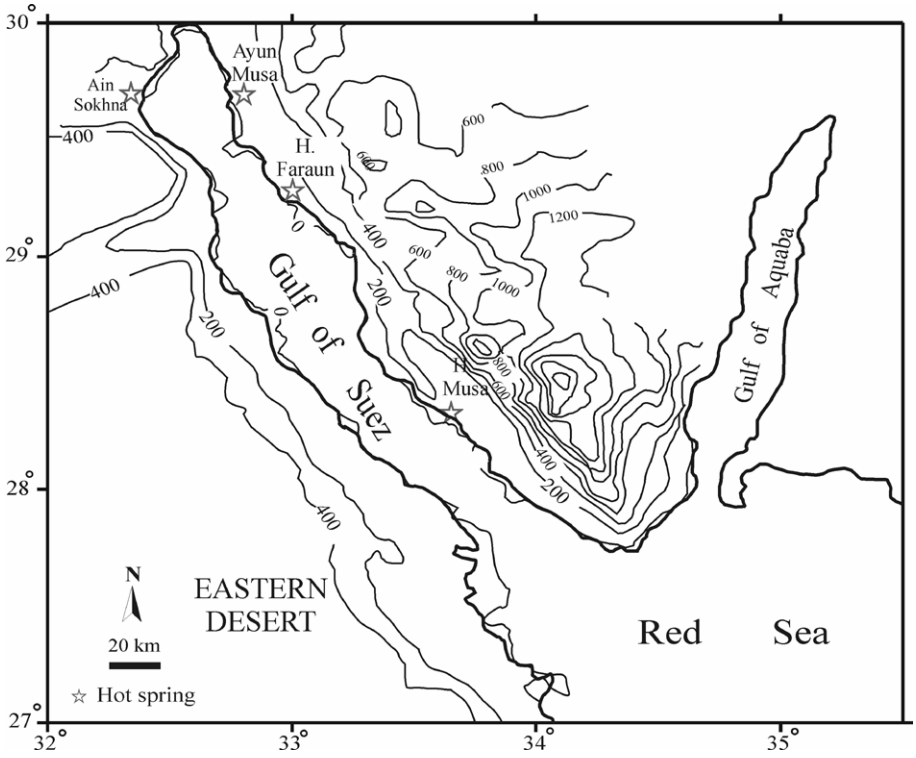

Fig. 1. Topography of the Gulf of Suez region [from GTOPO30 data set (Geschet et al., 1999)], showing the locations of the hot springs on the eastern and western margins of the Gulf.

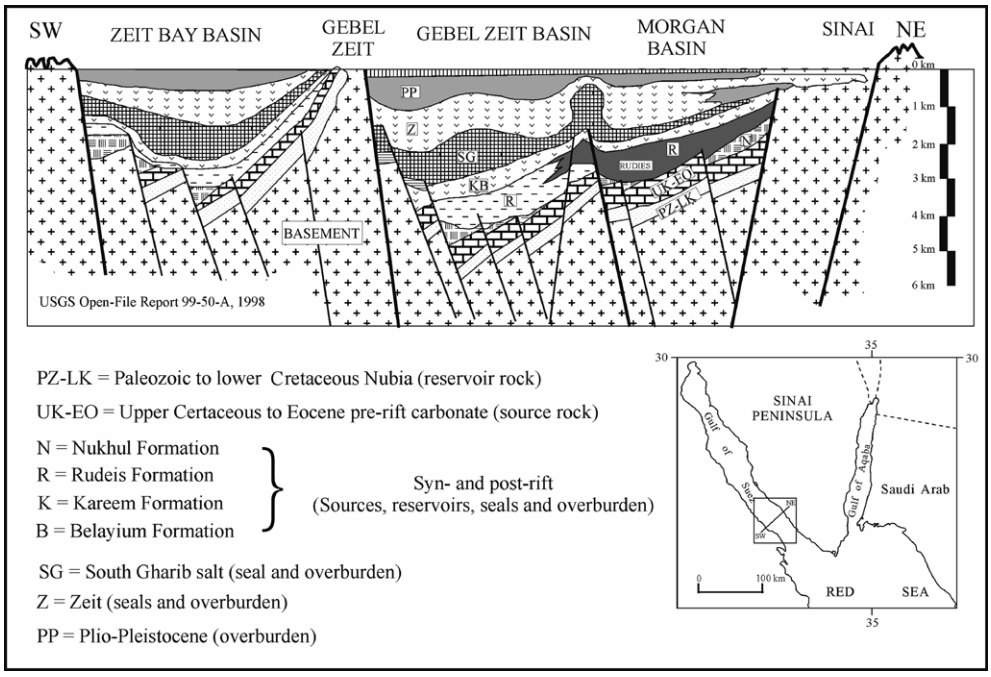

Fig. 2. Generalized structural cross section in the central Gulf of Suez, showing varying lithologies and depositional facies ranging from carbonate build-ups and deep submarine to terrigenous clastics [(United States Geological Survey (USGS), 1998].

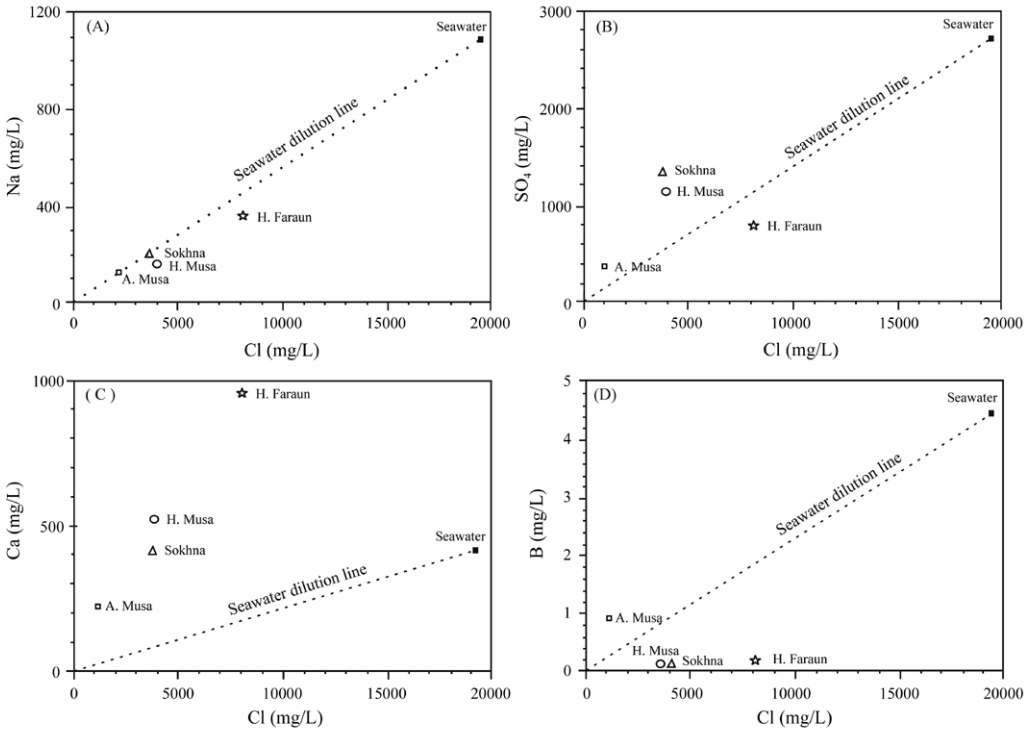

Fig. 3. Chloride variation diagrams for Gulf of Suez thermal waters (Hammam Faraun, Hammam Musa, Ayoun Musa and Ain Sokhna) compared with seawater dilution line (dashed line).

minerals such as calcite and gypsum from surrounding and overlain upper Cretaceous and Eocene carbonate rocks. Almost all thermal waters have a low concentration of boron (Fig. 3D) and this depletion may argue against direct sea water mixing in these areas. However, boron can be absorbed from groundwater onto clay minerals (Palmer et al., 1987).

The ratio of $^{3}He/^{4}He$ was recorded to be 0.256 times of the atmospheric ratio (R_{atm}) in the gases emitted from Hammam Faraun hot spring while this ratio equals 8 times of R_{atm} in the mantle. Hence, this ratio indicates that there is excess of helium (3.2%) which may be attributed to a deeper source of mantle (Sano et al. 1988). Sturchio and Arehart (1996) related such mantle He to the alteration in the subsurface due to late Tertiary volcanic eruptions.

Prediction of the scaling tendencies from geothermal waters is important in evaluating the production characteristics of geothermal aquifers and for taking necessary precautions to prevent or control scale formation. Assessment of scaling tendencies involves calculation of the saturation state of the scale forming minerals. MinteqA2 Ver. 4.0 computer code (HydroGeologic, Inc. and Allison Geoscience Consultants, Inc., 1999) was used to calculate saturation indices of the four hot spring waters. The results are listed in Table 2. All of the hot waters are undersaturated with respect to lime (calcium oxide). The waters closely approach the equilibrium with gypseum and celestite. All the waters are oversaturated with respect to calcite, aragonite, chrysotile, vaterite, sepiolite, dolomite except for Ayun Mussa hot spring. Ayun Mussa hot spring is especially oversaturated with fluorite. All the samples are oversaturated with respect to quartz.

The saturation states of thermal waters with respect to selected minerals suggest that carbonate minerals (calcite, aragonite and dolomite) are most likely to be precipitated as scales from the primary geothermal waters of Egypt during geothermal exploitation and well production. Additionally silica polymorphs (silica and chalcedony) seem to be precipitated during production applications.

4 Chemical geothermometers

The temperature of a geothermal reservoir can be measured directly or it can be estimated by chemical geothermometer calculations based on water chemistry. Studies of Na, K and Ca in aqueous systems suggest that cation concentrations are controlled by temperature-dependent equilibrium reactions with feldspars, mica and calcite. Several semi-empirical equations for the temperature have been determined on the basis of cation ratios ($\times 10^{-6}$). Several chemical geothermometers have been applied to the Gulf of Suez hot springs and the results are given in Table 3.

Table 1 Chemical data for Gulf of Suez thermal waters (mg/L) (Sturchio and Arehart, 1996)

	Ain Sokhna	Ayun Musa	Hammam Faraun	Hammam Musa
T(℃)	32	37	70	48
pH	7.74	6.02	7.44	7.59
SiO_2	19.1	17.8	51.1	21.6
B	0.04	0.90	0.18	0.04
Li	0.11	0.09	0.32	0.12
Na	1946	652	3642	1586
K	72.2	38.9	127	64.2
Mg	258	52.2	270	330
Ca	413	224	966	523
Sr	16.3	4.85	21.9	10.1
HCO_3	200	243	109	116
SO_4	1320	378	780	1130
F	2.4	6.6	2.5	1.6
Cl	3710	983	8050	3870
Br	14	6.3	46	31
T.D.S	7960	2600	14030	7670
$^{87}Sr/^{86}Sr$	0.70803	0.70776	0.70795	0.70795

The reservoir temperatures computed from the cation geothermometers for each water are generally higher than those of silica geothermometers, and this could be explained by silica precipitation due to cooling and boiling phenomena. It is obvious that Na-K geothermometers give anomalously high temperatures and suggest a deeper reservoir. The Na-K-Ca geothermometer measured temperatures are lower than those measured by using Cationic Composition Geothermometer (CCG), which is due to slightly high Mg contents in the sample. The Mg levels in high temperature geothermal fluids are usually very low (0.01 to 0.1 mg/L) (Nicholson, 1993), while in the Egyptian water samples, the Mg content ranges between 52.2 (Ayun Mussa) and 330 mg/L (Hammam Mussa). The high Mg concentrations can indicate near-surface reactions that leach Mg from the local rock or dilution by Mg-rich groundwater (Nicholson, 1993).

A further evaluation of the cation geothermometers is made on the Na-K-Mg diagram proposed by Giggenbach (1988). Fig. 4 shows that none of the Gulf of Suez thermal waters attains a water-rock chemical equilibrium, which indicates a partial equilibrium with the host rock and a possible mixing of different water types (Barragán et al., 2001). Hammam Faraun hot spring is the only water located close to the boundary between mature (partly equilibrated) and immature waters, therefore, temperature estimation can be performed with some degree of confidence.

Table 2 Saturation indices of the four kinds of hot spring water

Mineral	Ain Sukhna	Ayun Musa	Hammam Faraun	Hammam Musa
Anhydrite	-0.724	-1.151	-0.719	-0.675
Aragonite	0.644	-0.952	0.806	0.562
Artinite	-3.873	-9.582	-2.849	-3.258
Brucite	-3.681	-7.343	-2.195	-2.906
$CaCO_3{\cdot}xH_2O$	-0.535	-2.113	-0.093	-0.541
Calcite	0.772	-0.840	0.717	0.625
Celestite	-0.271	-0.973	-0.715	-0.616
Chalcedony	0.062	-0.026	0.119	-0.053
Chrysotile	0.654	-10.804	3.208	1.841
Cristobalite	-0.140	-0.228	-0.088	-0.257
Dolomite (disordered)	1.275	-2.299	1.371	1.241
Dolomite (ordered)	1.797	-1.795	1.763	1.705
Epsomite	-3.017	-3.92	-3.748	-3.126
Fluorite	-0.009	0.952	-0.212	-0.526
Gypsum	-0.510	-0.958	-0.664	-0.532
Halite	-3.912	-4.874	-3.447	-4.019
Huntite	-0.475	-8.012	-0.367	-0.412
Hydromagnesite	-8.251	-19.887	-7.096	-7.439
KCl	-4.931	-5.663	-4.439	-4.971
LiF	-6.351	-5.847	-6.125	-6.593
Lime	-18.985	-21.996	-15.613	-17.53
Magnesite	-0.333	-2.455	-1.288	-0.717
$Mg(OH)_2$ (active)	-5.833	-9.810	-6.508	-6.030
$Mg_2(OH)_3Cl{\cdot}4H_2O$	-8.961	-15.713	-9.724	-9.191
$MgCO_3{\cdot}5H_2O$	-3.181	-5.242	-3.765	-3.394
MgF_2	-2.712	-2.113	-2.86	-3.018
Mirabilite	-4.211	-5.619	-5.671	-5.181
NaF	-4.892	-4.766	-4.776	-5.227
Natron	-6.587	-9.144	-7.865	-7.643
Nesquehonite	-2.950	-4.946	-3.072	-2.957
Periclase	-8.014	-11.575	-5.82	-6.921
Portlandite	-9.254	-12.444	-7.121	-8.356
Quartz	0.501	0.406	0.508	0.364
Sepiolite	0.39	-7.346	2.493	1.129
Sepiolite (A)	-3.088	-11.139	-3.148	-3.322
SiO_2 (am, gel)	-0.755	-0.827	-0.59	-0.822
SiO_2 (am, $\times10^{-12}$)	-0.730	-0.805	-0.587	-0.806
SrF_2	-4.087	-3.339	-4.369	-4.814
Strontianite	-0.235	-2.117	-0.698	-0.758
Thenardite	-5.274	-6.449	-5.04	-5.489
Thermonatrite	-8.212	-10.57	-8.029	-8.618
Vaterite	0.235	-1.353	0.458	0.18

Note: All kinds of the thermal water are undersaturated with respect to lime (calcium oxide) and closely approach the equilibrium with gypseum and celestite. Moreover, all kinds of water are oversaturated with respect to calcite, aragonite, and dolomite except for Ayun Mussa hot spring.

5 Stable isotopes analysis

Isotopes are forms of a given chemical element that have different atomic masses. For a particular element, the isotopes have the same numbers of protons, and so have the same atomic number. However, each isotope has a different number of neutrons and therefore has a different atomic mass. Stable isotopes are those isotopes that do not undergo radioactive decay; so their nuclei are stable and their masses remain the same. However, they may themselves be the product of the decay of radioactive isotopes. The stable isotopes of ^{18}O (oxygen-18) and ^{2}H (deuterium) are used to provide information on hydrological processes, including groundwater-surface water interactions. Isotope variations are small and fractional differences (δ) are expressed as the parts per thousand difference of the ratio of the heavy isotope to the light isotope of the sample relative to a standard, as follows,

$$\delta_{\text{sample}} = \frac{R_{\text{sample}} - R_{\text{standard}}}{R_{\text{standard}}} \times 1000 \quad (1)$$

Table 3 Geothermometry results of hot spring waters (℃)

	A	B	C	D	E	F
Ain Sukhna	32	164.78	61.86	95.04	53.53	32.76
Ayun Musa	37	164.13	59.14	109.7	50.77	29.92
Hammam Faraun	70	128.29	140.7	91.53	97.55	78.77
Hammam Musa	48	163.79	66.66	95.53	58.45	37.84

Note: A. Emergence temperature (℃); B. CCG (Nieva & Nieva, 1987); C. Na-K (Fournier and Truesdell, 1979); D. Na-K-Ca (Fournier and Truesdell, 1973); E. Silica (Verma, 2000).

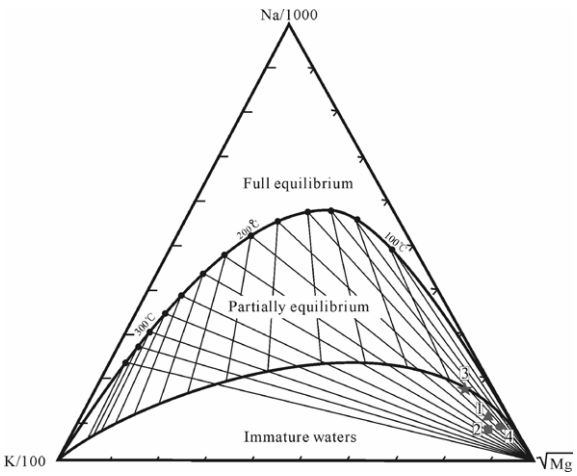

Fig. 4. Ternary diagram of the water-rock equilibration temperatures as modified from (Giggenbach, 1988) using relative Na, K, and Mg concentrations of the Gulf of Suez thermal waters. 1 = Ain Sokhna; 2 = Ayun Musa; 3 = Hammam Faraun; 4 = Hammam Musa.

Samples from the hot waters were collected and stable isotopes of ^{18}O and deuterium were measured and listed in Table 4. Oxygen and hydrogen isotope compositions are commonly reported relative to an agreed sample of ocean water, referred to as the standard mean ocean water (SMOW), representing the largest and most equilibrated water body. Stable isotope ratios of deuterium/hydrogen ($^{2}H/^{1}H$) and $^{18}O/^{16}O$

of water are conventionally expressed as units of parts per thousand deviations from SMOW. Based on about 400 water samples from rivers, lakes and precipitation, a linear relationship between deuterium and oxygen-18 was established for average global meteoric waters. This relationship ($\delta D = 8\delta^{18}O + 10$) is known as the Global Meteoric Water Line (GMWL) and provides a useful benchmark against which regional or local waters can be compared and their isotopic composition can be interpreted. Comparison of the stable isotope data for surface water samples of hot springs relative to the global or local meteoric water lines can provide information on the origin of these hot springs (Fig. 5).

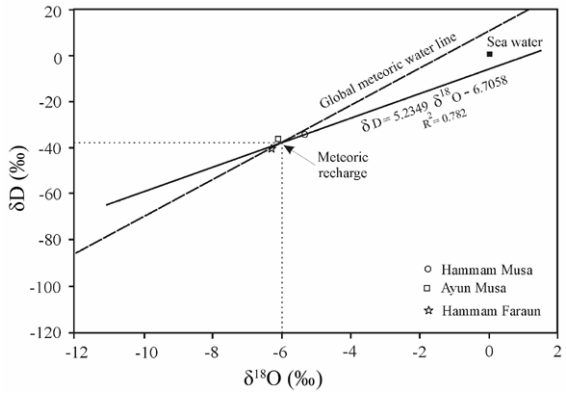

Fig. 5. δD ‰ vs. $\delta^{18}O$ ‰ in thermal waters of Hammam Musa, Ayun Musa and Hammam Faraun hot springs. The relationship $\delta D = 5.23\ \delta^{18}O - 6.7$ represents the local meteoric water of the area of Gulf of Suez.

Table 4 Stable isotopic analysis for the thermal water of Ayun Musa, Hammam Faraun and Hammam Musa hot springs

No.	Sample name	Sampling date	$\delta^{18}O$ (‰)	δD (‰)
1	Ayun Musa	2008/12/20	-6.0	-36.9
2	Hammam Faraun	2008/12/20	-6.2	-40.3
3	Hammam Musa	2008/12/19	-5.4	-35.0

6 Conceptual Geochemical model for the hottest spring in Egypt

The most important area for geothermal manifestation is located in the Hammam Faraun hot spring, which represents the hottest spring in Egypt (Morgan et al., 1983). The Hammam Faraun tilted block is one of the main fault blocks in the central dip province of the Suez rift, and it is bound on the east and west by major normal fault zones. The shallow geological succession in the Hammam Faraun area is distinguished by sand, conglomerate, sandy limestone, lagoonal gypsum limestone, salty limestone and chalk with flinty limestone. This succession varies with age from post Pliocene, Pliocene, Miocene, Oligocene, Eocene and upper Cretaceous, respectively (Jackson et al., 2002) (Fig. 6). The Hammam Faraun hot spring (70℃) issues from faulted dolomitic Eocene limestone.

Conceptual geochemical model was made at Hammam Faraun hot spring and indicates that derivation of solutes is mainly from regional marine sedimentary rocks (Fig. 6). The abundance of Ca relative to the seawater dilution suggests the presence of Ca minerals such as calcite or gypsum; their possible sources are the upper Cretaceous and Eocene carbonate rocks overlying the Nubian sandstone, windblown deposits in the recharge area, and gypsum from Miocene evaporates and marine aerosols. The enrichment of chlorite may derive from sea water intrusion in that area. In addition, the abundance of SO_4 may indicate excess Ca was derived from the dissolution of gypsum.

The geochemical and isotopic compositions of Hammam Faraun hot spring indicate that the source of the hot springs is due to deep fluid circulation through faults on the surface of the basement rock. These faults allow the formation of discharge conduits for water ascending from depth after being heated and mixed with other water types.

7 Conclusions

The geological and structure setting of Egypt reflect that the most areas for geothermal exportation are located in the eastern side of Egypt adjacent to Red Sea and Gulf of Suez. Chemical and isotopic analyses of thermal waters of the main hot springs in the areas around Gulf of Suez were made by Sturchio and Arehart (1996). The most abundant solutes in all thermal waters are Na and Cl, while Mg, Ca, and SO_4 also are prominent and the pH values are near neutral, indicating that derivation of solutes is mainly from regional marine sedimentary rocks. Stable isotope ratios of deuterium/hydrogen ($^2H/^1H$) and $^{18}O/^{16}O$ of samples that collected from the Gulf of Suez hot springs, reflecting that the main recharge of the hot springs come from meteoric water with minor intrusion of sea water.

Acknowledgements The authors are grateful to the members of Geothermic Laboratory, Earth Resource Engineering Department, and Kyushu University for their cooperation. We also acknowledge the stuff of National Research of Astronomy and Geophysics, Egypt for their continuous support and help.

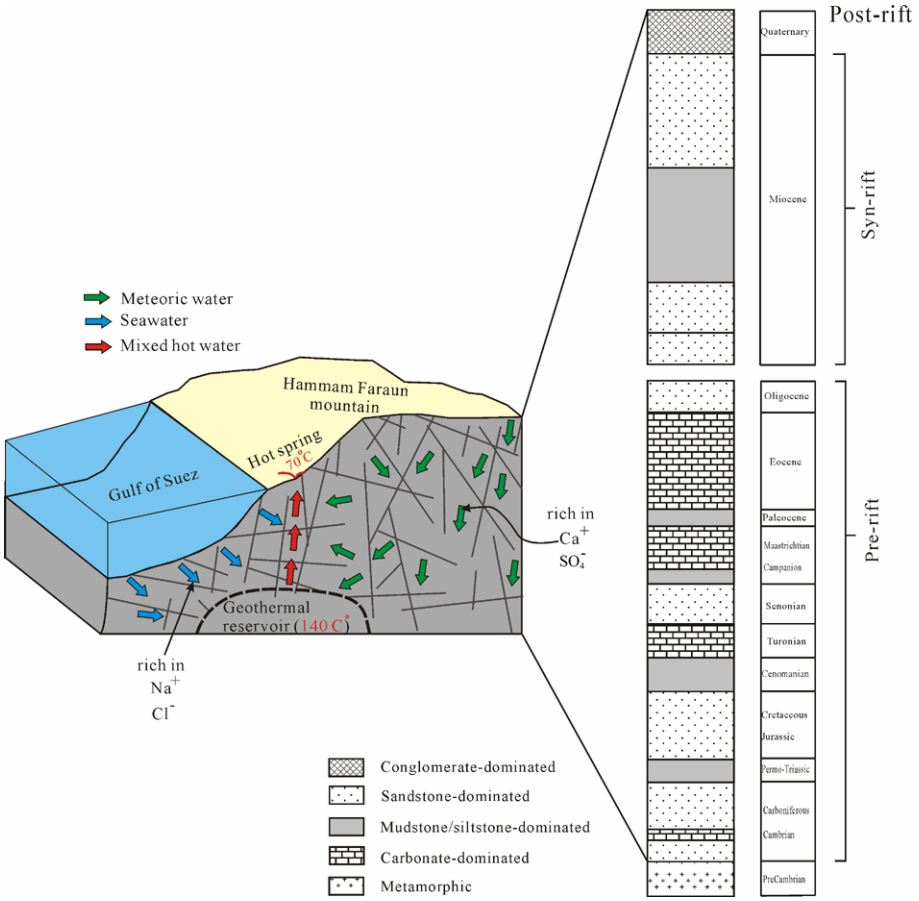

Fig. 6. Schematic diagram shows the conceptual geochemical model of the hydrothermal system in the Hammam Faraun hot spring. The groundwater is ascending from depth after being heated and mixed with other water types. The simplified stratigraphy of the area of Hammam Faraun was modified after Jackson et al. (2002).

References

Barragán R.M., Arellano V.M., Portugal E., Sandoval F., and Barrera V.M. (2001) Gas equilibrium for the Los Azufres (Michoacán) geothermal reservoir, México. In *Proceedings of the 22nd PNOC-EDC Geothermal Conference* [M]. pp.81−87. Manila, Philippines.

Colletta B., Le Quellec P., Letouzey J., and Moretti I. (1988) Longitudinal evolution of the Suez rift structure (Egypt) [J]. *Tectonophysics*. **153**, 221–233.

Davisson M.L., Presser T.S., and Criss R.E. (1994) Geochemistry of tectonically expelled fluids from the northern Coast Ranges, Rumsey Hills, California, USA [J]. *Geochim. et Cosmochim Acta*. **58**, 1687–1699.

El Kiki F.E., Mabrook B., and Swailem F.M. (1978) Evaluation of trace elements and tritium content in some mineral springs in Egypt [J]. *Isotope & Rad. Res*. **10**, 55–82.

Evans A.L. (1988) Neogene tectonic and stratigraphic events in the Gulf of Suez rift area, Egypt [J]. *Tectonophysics*. **153**, 235–247.

Fournier R.O. and Potter R.W. (1979) Magnesium correction to Na-K-Ca chemical geothermometer [J]. *Geochim. et Cosmochim. Acta*. **43**, 1543–1550.

Fournier R.O. and Truesdell A.H. (1973) An empirical Na-K-Ca geothermometer for natural waters [J]. *Geochim. et Cosmochim. Acta*. **37**, 1255–1275.

Garfunkel Z. and Bartov Y. (1977) The tectonics of the Suez Rift [J]. *Geol. Surv. Isr. Bull*. **71**, 44.

Gesch D.B., Verdin K. L., and Greenlee S.K. (1999) New land surface digital elevation model covers the Earth [J]. *Eos. Trans. AGU*. **80**, 69–70.

Giggenbach W.F. (1988) Geothermal solute equilibria: Derivation of Na–K–Mg–Ca geoindicators [J]. *Geochim. et Cosmochim. Acta*. **52**, 2749–2765.

Himida I.H., Bishay N.Z., and Diab M. S. (1972) Hydrogeological and hydrogeochemical studies on Ayun Musa area [J]. *Desert Institute Bulletin*. **22**, 17–32.

HydroGeoLogic, Inc., and Allison Geoscience Consutants, Inc. (1999) *MINTEQA2/PRODEFA2, A Geochemical Assessment Model for Environmental Systems: User Manual Supplement for Version 4.0*. [Z]. HydroGeoLogic, Inc., and Allison Geoscience Consutants, Inc.

Issar A., Rosenthal Y., and Eckstein R.B. (1971) Formation waters, hot springs and mineralization phenomena along the eastern shore of the Gulf of Suez [J]. *International Association of Scientific Hydrology*. **14**,

25–44.

Jackson C.A.L., Gawthorpe R.L., and Sharp I.R. (2002) Growth and linkage of the East Tanka fault zone; structural style and syn-rift stratigraphic response [J]. *Journal of the Geological Society of London*. **159**, 175–187.

McKenzie D.P., Davies D., and Molnar P. (1970) Plate Tectonics of the Red Sea and East Africa [J]. *Nature.* **226**, 243–248.

Meneisy M.Y. and Kreuzer H. (1974) Potassium-argon ages of Egyptian basaltic rocks [J]. *Geol. Jahrb.* **D9**, 21–31.

Morgan P., Boulos K., and Swanberg C.A. (1983) Regional geothermal exploration in Egypt [J]. *Geophysical Prospecting*. **31**, 361–376.

Nicholson, K. (1993) *Geothermal Fluids: Chemistry and Exploration Techniques* [M]. pp.253. Springer-Verlag, Berlin Heidelberg.

Nieva and R. Nieva (1987) Developments in geothermal energy in Mexico. Part twelve: a cationic geothermometer for prospecting of geothermal resources [J]. *Heat Recov. Syst.* **7**, 243–258.

Palmer M.R., Spivack A.J., and Edmond J.M. (1987) Temperature and pH controls over isotopic fractionation during adsorption of boron on marine clay [J]. *Geochim. et Cosmochim. Acta.* **51**, 2319–2323.

Patton T.L., Moustafa A.R., Nelson R.A., and Abdine A.S. (1994) Tectonic evolution and structural setting of the Suez rift. In *Interior Rift Basins. Am. Assoc. Pet. Geol. Mem*. (ed. Landon S.M.) [M]. **58**, 9–55.

Said R. (1962) *Geology of Egypt* [M]. pp.377. Elsevier, Amsterdam.

Sano Y., Nakamura Y., Notsu K., and Wakita H. (1988) Influence of volcanic eruptions on helium isotope ratios in hydrothermal systems induced by volcanic eruptions [J]. *Geochim. et Gosmochim. Acta.* **52**, 1305–1308.

Schütz K.I. (1994) Structure and Stratigraphy of the Gulf of Suez, Egypt. In *Interior Rift Basins, AAPG Memoir 59* (ed. Landon S.M.) [M]. pp.57−96. The American Association of Petroleum Geologists, Tulsa, Oklahoma, USA.

Sellwood B.W. and Netherwood R.E. (1984) Facies evolution in the Gulf of Suez area: sedimentation history as an indicator of rift initiation and development [J]. *Mod. Geol.* **9**, 43–69.

Shata A.A. (1990) *Thermal Springs and Mineralized Water in the Gulf of Suez Taphrogenic Basin, Northeast Egypt* [R]. pp.681−688. Memoires of the 22nd Congress of IAH, XXII, Lausanne.

Siedner G. (1973) K-Ar chronology of Cenozoic volcanic from northern Israel and Sinai [J]. *Fortschr. Mineral.* **50**, 129–130.

Sturchio N.C. and Arehart G.B. (1996) Composition and origin of thermal waters in the Gulf of Suez area, Egypt [J]. *Applied Geochemistry*. **2**, 471–479.

United States Geological Survey, USGS (1998) *The Red Sea Basin Province* [Z]. Open File No.99−50−A. United States Geological Survey, Washington.

Verma M.P. (2000) *Revised Quartz Solubility Temperature Dependence Equation Along the Water-vapor Sauration Curve* [R]. pp.1927−1932. World Geothermal Congress, Kyushu-Tohoku, Japan.